

A Well-Defined Osmium-Cupin Complex: Hyperstable Artificial Osmium Peroxygenase

Nobutaka Fujieda, Takumi Nakano, Yuki Taniguchi, Haruna Ichihashi, Hideki Sugimoto, Yuma Morimoto, Yosuke Nishikawa, Genji Kurisu, and Shinobu Itoh

J. Am. Chem. Soc., **Just Accepted Manuscript** • DOI: 10.1021/jacs.7b00675 • Publication Date (Web): 24 Mar 2017

Downloaded from <http://pubs.acs.org> on March 26, 2017

Just Accepted

“Just Accepted” manuscripts have been peer-reviewed and accepted for publication. They are posted online prior to technical editing, formatting for publication and author proofing. The American Chemical Society provides “Just Accepted” as a free service to the research community to expedite the dissemination of scientific material as soon as possible after acceptance. “Just Accepted” manuscripts appear in full in PDF format accompanied by an HTML abstract. “Just Accepted” manuscripts have been fully peer reviewed, but should not be considered the official version of record. They are accessible to all readers and citable by the Digital Object Identifier (DOI®). “Just Accepted” is an optional service offered to authors. Therefore, the “Just Accepted” Web site may not include all articles that will be published in the journal. After a manuscript is technically edited and formatted, it will be removed from the “Just Accepted” Web site and published as an ASAP article. Note that technical editing may introduce minor changes to the manuscript text and/or graphics which could affect content, and all legal disclaimers and ethical guidelines that apply to the journal pertain. ACS cannot be held responsible for errors or consequences arising from the use of information contained in these “Just Accepted” manuscripts.

A Well-Defined Osmium-Cupin Complex: Hyperstable Artificial Osmium Peroxygenase

Nobutaka Fujieda,^{a,*} Takumi Nakano,^a Yuki Taniguchi,^a Haruna Ichihashi,^a Hideki Sugimoto,^a Yuma Morimoto,^a Yosuke Nishikawa,^b Genji Kurisu,^b and Shinobu Itoh^{a,*}

^aDepartment of Material and Life Science, Graduate School of Engineering, Osaka University, 2-1 Yamada-oka, Suita, Osaka 565-0871, Japan

^bInstitute for Protein Research, Osaka University, 3-2 Yamada-oka, Suita, Osaka 565-0871, Japan

ABSTRACT: Thermally stable TM1459 cupin superfamily protein from *Thermotoga maritima* was repurposed as an osmium (Os) peroxygenase by metal-substitution strategy employing the metal-binding promiscuity. This novel artificial metalloenzyme bears a datively bound Os ion supported by the 4-histidine motif. The well-defined Os center is responsible for not only the catalytic activity but also the thermodynamic stability of the protein folding, leading to the robust biocatalyst ($T_m \approx 120$ °C). The spectroscopic analysis and atomic resolution X-ray crystal structures of Os-bound TM1459 revealed two types of donor sets to Os center with octahedral coordination geometry. One includes *trans*-dioxide, OH, and *mer*-three histidine imidazoles (O_3N_3 donor set), whereas another one has four histidine imidazoles plus OH and water molecule in a *cis* position (O_2N_4 donor set). The Os-bound TM1459 having the latter donor set (O_2N_4 donor set) was evaluated as a peroxygenase, which was able to catalyze *cis*-dihydroxylation of several alkenes efficiently. With the low catalyst loading (0.01% mol), up to 9100 turnover number was achieved for the dihydroxylation of 2-methoxy-6-vinyl-naphthalene (50 mM) using an equivalent of H_2O_2 as oxidant at 70 °C for 12 h. When octene isomers were dihydroxylated in a preparative scale for 5 h (2 % mol cat.), the terminal alkene octene isomers was converted to the corresponding diols in a higher yield as compared with the internal alkenes. The result indicates that the protein scaffold can control the *regio*-selectivity by the steric hindrance. This protein scaffold enhances the efficiency of the reaction by suppressing disproportionation of H_2O_2 on Os reaction center. Moreover, upon a simple site-directed mutagenesis, the catalytic activity was enhanced by about three-fold, indicating that Os-TM1459 is evolvable nascent osmium peroxygenase.

INTRODUCTION

To meet industrial demands,¹ tremendous efforts have been recently made to develop highly *regio*- and/or *stereo*(*enantio*)-selective artificial metalloenzymes by combining a biomolecule (protein/DNA) with a synthetic metal complex.²⁻⁴ For the purpose of linking of a protein matrix and a metal complex, various strategies have been pursued including covalent attachment, supramolecular interaction, and dual linking methods of them with dative anchoring by the amino acid residues to the metal center of complex.⁵⁻¹¹ Although the rates of the reactions catalyzed by these systems have been much slower than those of natural enzymes, Ward group and Hartwig group demonstrated that artificial metalloenzymes could be controlled by genetic manipulation of the protein scaffold¹² and consequently possess the fundamental characteristics of natural enzymes.^{13,14} On the other hand, the another approach has been employed based on the direct complexation of bare metal ions with either natural¹⁵ or non-natural¹⁶ amino acids as the ligands. More recently, the enzyme repurposing's have been revealed to be promising, via self-assembly of monomeric protein¹⁷ and by exploring the latent metal binding site.¹⁸ Far more well-organized strategy

is the metal-substitution of natural metalloenzymes based on their metal binding promiscuity to generate novel activity.^{19,20}

There are several lines of evidence that the replacement of copper center of blue copper protein by Hg^{II} and Cd^{II} can lead to the large thermal stabilization of protein folding because of stronger donor-acceptor combination (soft donor (Cys and Met) and soft metal ion) and their strong coordination bond of heavy metal ion.²¹ Thus, the replacement of native metal ion to preferable different metal ion will be one of powerful methods to endow the protein scaffold with robustness as well as novel catalytic capability. In this context, platinum-group elements (Ru, Os, Rh, Ir, Pd, and Pt) might be suitable for this purpose, although these elements are hardly employed in natural enzymes due to their scarcity in usual environments.

Independently, Kazlauskas group²² and Soumillion group²³ have accomplished the metal replacement of 3-His metal binding site of carbonic anhydrase, that is a Zn-containing hydrolase, by Mn to create a *stereo*-selective alkene epoxidase. Kazlauskas group further developed this strategy by employing Rh ion to create a *stereo*-selective alkene hydroxylase²⁴ and a *regio*-selective hydroformylase.²⁵ Hartwig

group report the efficient synthesis of organometallic complexes with this hydrolase.²⁶ These results demonstrate that such methodology is promising for construction of biocatalysts. However, the elimination of non-specific binding of Rh ion to other His residues seems to be fairly difficult.^{24,25} By and large, the precise interaction and location of metal binding is rarely established.

In this study, we have succeeded to develop a nascent mononuclear osmium enzyme with a *cupin*-type fold, where *well-defined* amino acid residues for Os-coordination are disposed in the small *cone-shaped cleft* of protein matrix. For this purpose, we employed the TM1459 gene from *Thermotoga maritima* encoding a homodimeric Mn-binding protein with a molecular weight of 12,977 Da (residues 1–114, Figure 1A).²⁷ Currently, the biological function of Mn-bound TM1459 (Mn-TM1459) has yet to be identified, although it was found to show the C=C bond cleavage activity in the presence of alkylperoxide as oxidant *in vitro*.²⁸ The metal binding site consists of 4-histidine residues in a similar geometry to that of the tris(2-pyridylmethyl)amine (TPA) ligand system (Figure 1BC), the Fe-complexes of which have been extensively studied as the model complexes of the active sites of nonheme metalloenzymes.²⁹ We have already achieved the efficient *cis*-1,2-dihydroxylation reactions with alkene derivatives by using Os-TPA complexes.³⁰ The several alkene dihydroxylation systems of Os ion with the protein molecule as additives have been reported.^{31–33} In all these cases, the turnover number (TON) and the *regio*-selectivity for the substrate are still limited. Moreover, straightforward redesign of the well-ordered catalytic- and substrate-binding site around metal center remains unachieved, because of non-specific binding of Os ions to protein surface as well.

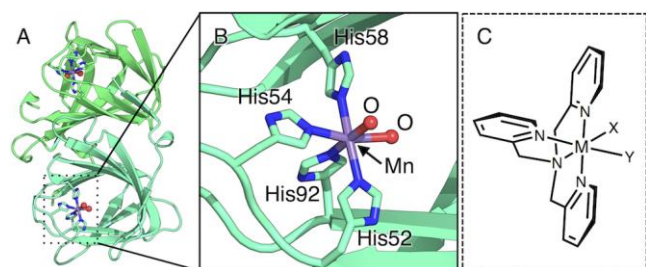


Figure 1. (A) The overall structure and (B) Mn center of TM1459 protein (PDB code: 1VJ2). (C) The schematic representation of TPA-metal complex

Herein, in a spirit of “chemomimetic biocatalysis”,^{34,35} we have developed an atom economic and selective *cis*-1,2-dihydroxylation reaction system by using thermostable protein as the ligand instead of TPA. Os-cupin (TM1459) complexes have characterized by X-ray crystallographic analysis at atomic resolution and spectroscopic methods, and their stabilities were confirmed by differential scanning calorimetry (DSC) and circular dichroism (CD) spectroscopy. In order to evaluate the chemical function of the Os-bound TM1459, the alkene dihydroxylation reaction with H₂O₂ has been examined in detail. Furthermore, the dihydroxylation reactivity of several mutants has been investigated to clarify whether the

catalytic activity of Os-bound TM1459 can be evolved by the amino acid alteration.

RESULTS AND DISCUSSION

Incorporation of Osmium Ion into Well-defined Metal Binding Site of Apo-TM1459. TM1459 was over-expressed in *E. coli* BL21(DE3) with the expression plasmid containing the rare codon-modified TM1459 gene (Table S1-S2 and Figure S1-S3) and isolated as homogenous state on SDS-PAGE (Figure S4). Its metal content was determined to be less than 0.02 metal ions (Mn, Fe, Co, Ni, Cu, Zn each) per protein subunits by the Inductively Coupled Plasma-Atomic Emission Spectrometry (ICP-AES) analysis, indicating that EDTA efficiently eliminated the contamination of metal ions in the wash step of affinity chromatography (see SI Experimental Section). The crystal structure of as-isolated TM1459 (apo-TM1459) was determined at 1.20 Å resolution by the molecular replacement method using the reported coordinate of Mn-TM1459 (Figure 1AB, PDB code: 1VJ2) as a search model (Table S3 and Figure S5).²⁷ The overall structure is nearly identical to the reported structure (chain A of the Mn-bound form vs chain A of apo-form, RMSD = 0.414 (98 C α atoms)).²⁷ No electron density corresponding to metal ions was observed in consistent with the results of ICP-AES analysis (Figure 2A).

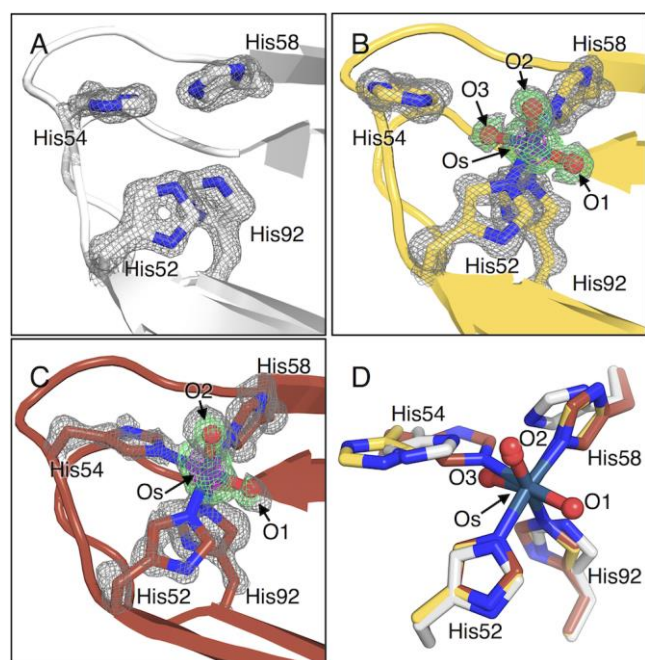


Figure 2. Closed view of the metal binding 4-histidine motif of atomic resolution crystal structures of TM1459s. (A) Apo-form, PDB code: 5WSD; (B) Form I, PDB code: 5WSE; (C) Form II, PDB code: 5WSF; (D) Superimposed structure of 4-histidine motif of three form (Apo vs Form I vs Form II). The protein main chain is displayed as ribbon and key amino acid residues are highlighted as sticks. $2F_o - F_c$ map, omit map ($F_o - F_c$), anomalous map contoured at 1.5, 4.0, and 8.0 σ are shown in gray, green, and magenta mesh, respectively. Omit map was calculated around Os and O center. Selected bonds, angles, and their estimated errors (Table S3–S6): Form I (Panel B, chain A), Os–N ϵ (His52), 2.11(0.02) Å; Os–N ϵ (His58), 2.09(0.02) Å; Os–N ϵ (His92), 2.10(0.02) Å; Os–O1, 1.76(0.02) Å; Os–O2, 1.88(0.02) Å; Os–O3, 1.77(0.02) Å; O1–Os–O3 168.2(0.8) $^\circ$; O2–Os–N ϵ (His92),

178.9(0.8)°, Form II (Panel C, chain C), Os–N ϵ (His52), 2.14(0.02) Å; Os–N ϵ (His54), 2.11(0.04) Å; Os–N ϵ (His58), 2.10(0.02) Å; Os–N ϵ (His92), 2.15(0.03) Å; Os–O1, 1.81(0.02) Å; Os–O2, 2.05(0.02) Å; O1–Os–O2 89.4(1.1)°; O2–Os–N ϵ (His92), 175.9(1.2)°; O1–Os–N ϵ (His54), 175.2(0.9)°.

The apo-TM1459 was incubated with 1.2 equivalents of $K_2[Os^{VI}(O)_2(OH)_4]$ for 4 days in 4-(2-hydroxyethyl)-1-piperazineethanesulfonic acid (HEPES) buffer at pH 7.0 and 70 °C under N_2 . The color of the solution (purple) has changed to yellow within 16 h and then gradually turned into reddish brown, suggesting presence of an intermediate (Figure S6A). In order to scrutinize this transformation, the yellow species (form I) and the reddish brown species (form II) were collected after 16 h and 96 h incubation, respectively, and were subjected to size-exchange chromatography to remove the excess amount of Os ions. The metal content of each species was determined to be 1.0 ± 0.1 Os ions per protein subunits by the ICP-AES analysis. The results suggested that both forms I and II accommodate an Os ion in each subunit. Then, the valence state and the coordination structures were examined as follows. Form I exhibited an absorption spectrum with poorly resolved shoulder peaks between 300 and 450 nm, whereas form II showed an absorption band at 373 nm (orange and red spectra, respectively, in Figure 3A). Furthermore, it's noteworthy to note that both form I and form II exhibited the broad ESR signal centered at $g = 2.1$ (Figure S6B). Whereas form I exhibited several additional minor signals was observed, there was no such signal in the case of form II (red spectrum in Figure S6B).

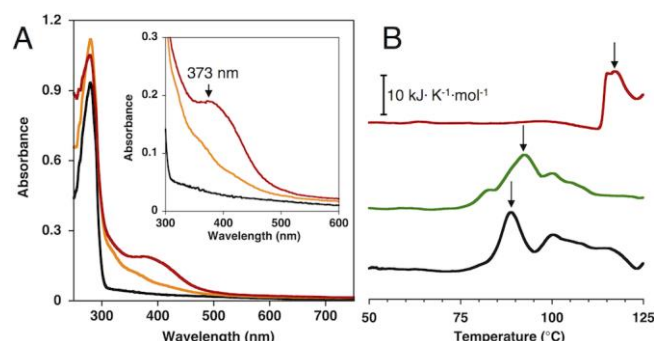


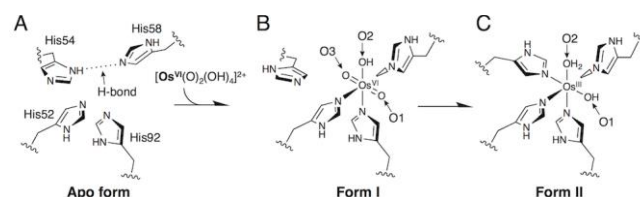
Figure 3. (A) UV-vis spectra of 0.1 mM apo-form (black), form I (orange), and form II (red) in 10 mM potassium phosphate buffer at pH 7.0 and room temperature. Inset: Extended UV-vis spectra of apo-form (black), form I (orange), and form II (red). (B) Calorimetric scans of apo-form (black), Mn-bound form (green), and Os-bound form (red) in 50 mM potassium phosphate buffer at pH 7.0.

Crystal Structures of Osmium-incorporated TM1459. For further information about form I and form II, the crystal structures of both Os-bound forms were determined at atomic resolution of 1.12 and 1.11 Å, respectively (Figure 2, Figure S7 and Table S3–S6). The overall structures of form I and form II are almost identical to that of the apo-form (Figure S7AB). In each chain of both form I and form II, one intense anomalous peak due to Os ion was found around the N ϵ atoms of His52, 58, and 92 (Figure 2BC, magenta mesh). In the form I crystal, the positions of imidazoles of His58 and His92 deviated from those of the apo-form because of the coordination to Os ion,

and the imidazole of His54 rotated further away due to the steric repulsion with the Os-coordinating O3 (Figure 2D). The coordinating three histidines have the metal-to-N distances of 2.11(0.02), 2.09(0.02), and 2.10(0.02) Å, respectively. Besides these N donors (one imidazole of His54 is uncoordinated), the Os center is ligated by three oxygen atoms taking an octahedral geometry. Two oxygen atoms (O1 and O3) with shorter Os–O distances (1.76(0.02) and 1.77(0.02) Å) and another oxygen atom (O2) with longer Os–O distance (1.88(0.02) Å) could be assigned to oxide and hydroxide ligands, respectively. From structural analogy to the reported *trans*-dioxide-Os^{VI}-tetrapyrazole complex,³⁶ the Os center in form I is likely to be a *trans*-dioxide-Os^{VI}(OH) species retaining its high-valency after complexation with three imidazole. This is consistent with the previous observation that the *trans*-dioxide-Os^{VI} is much more stable as compared to the *cis*-dioxide-Os^{VI}.³⁷

In stark contrast, in form II crystal, the Os center is supported by four histidine residues (His52, 54, 58, and 92) with metal-to-N distances of 2.14(0.02), 2.11(0.03), 2.10(0.02), and 2.15(0.03) Å, respectively (Figure 2C). Thus, the imidazole ring of His 54 flipped toward the Os center (O3 position in the form I crystal) and rotated away from the mouth of cavity in the crystals of form I and apo-form (Figure 2D). Further structural inspection lead to identification of the two labile sites in a *cis*-position occupied by two oxygen atoms, taking octahedral geometry. According to the bond length (2.05(0.02) and 1.81(0.02) Å), one oxygen atom (O2) could be water molecule and the other one (O1) could be hydroxide ion. This coordination geometry is reminiscent of the structure of $[Os^{III}(H_2O)(OH)(TPA)]^{2+}$ complex, UV-vis spectrum of which shows the peak at 350 nm, that is similar to that of form II (373 nm, Figure 3A).³⁰ In the reported Mn-bound structure, the distances of water molecules to Mn ion are 2.24 (Mn–O1) and 2.06 (Mn–O2) Å, which are significantly longer than that of Os–O1 in form II (Figure S7E), supporting the assignment of O1 as an hydroxide oxygen.²⁷ Taken together, Os ion initially attaches to the three His imidazoles (His52, 58, and 92) with keeping the Os^{VI} oxidation state and the *trans*-dioxide geometry (form I, Scheme 1B). Then both oxide oxygens as well as Os^{VI} are reduced during the incubation at 70 °C for 4 days to Os^{III}, hydroxide, and water molecule, respectively, and ligand replacement occurs concomitantly (form II, Scheme 1C). To avoid confusion of these two forms (form I and II), hereafter, form II (reddish brown species) is called as Os-TM1459.

Scheme 1. Schematic Representation of $[Os^{VI}(O)_2(OH)_4]^{2+}$ Incorporation in Apo-form of TM1459 Protein



Stability of Os-TM1459. The stability of apo-, Mn- and Os-TM1459 is examined by DSC analysis (Figure 3B). Apo-, Mn-, and Os-TM1459 exhibited the several overlapping transitions. Since all of these forms didn't show any reversible profiles due to the corresponding refolding transitions in the reverse

1 scan, it was difficult to determine detailed thermodynamic
2 parameters. Thus, the maximum peaks at 87, 93, and 117 °C
3 were used for rough estimation of the apparent denaturation
4 temperature (T_m) of apo-, Mn-, and Os-TM1459, respectively
5 (Figure 3B, arrows). The observed peak shifts toward higher
6 temperature indicated that the protein folding was thermally
7 stabilized upon the metal binding to the apo-form. The value
8 of ΔT_m (apparent denaturation temperature difference be-
9 tween the metal-binding form and the apo-form) of Mn-
10 TM1459 and Os-TM1459 are 6 and 30 °C, respectively. These
11 ΔT_m values reflect the strength of the metal binding as is
12 reported in the case of transferrin and cupredoxin.^{21,38} The Δ
13 T_m value of Os-TM1459 (30 °C) is much higher than that of
14 Mn-TM1459 (6 °C), suggesting that the binding of Os ion to
15 the protein is much stronger than that of Mn ion. Indeed, Os-
16 N ϵ (imidazole) bonds (average 2.11 Å) in Os-TM1459 are fairly
17 shorter than Mn-N ϵ (imidazole) bonds (average 2.21 Å) in
18 Mn-TM1459.

19 For native metalloproteins, a representative ΔT_m value has
20 been reported as 8 °C for Zn^{II}-carbonic anhydrase.³⁹ Even
21 though higher values around 20 °C have been known for Cu^{II}-
22 cupredoxin⁴⁰ and Fe^{III}-transferrin,³⁸ the ΔT_m values were fur-
23 ther increased upon replacing by xenobiotic Hg^{II} and Cd^{II} (29
24 and 31 °C, respectively).²¹ The result could be explained by the
25 fact that soft donor atoms such as sulfur of Cys and Met bind
26 to softer metal ions such as Hg^{II} and Cd^{II} stronger than harder
27 metal ions such as Cu^{II} and Fe^{III}. On the other hand, the large
28 ΔT_m value of Os-TM1459 (30 °C) can be attributed to the
29 strong Os–N ϵ (imidazole) bonding due to strong back electron
30 donation from the Os center to the imidazole π -orbital as in
31 the case of Os^{III}-TPA complex.⁴¹

32 Besides the high thermal stability, chemical stability of Os-
33 TM1459 was also improved as confirmed by the CD meas-
34 urements under various conditions. Namely, the contents of
35 secondary structure of Os-TM1459 hardly changed under
36 both acidic and alkaline conditions (pH 2–10) even in the
37 presence of high concentration of organic solvents (50 % v/v
38 *t*-butylalcohol (*t*-BuOH), Figure S8).

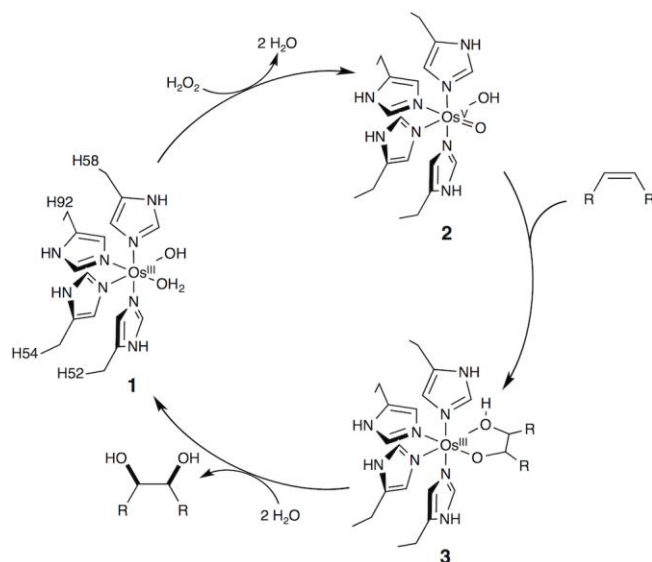
39 **Peroxygenase Activity of TM1459.** The catalytic activity of
40 Os-TM1459 was examined for the alkene dihydroxylation
41 using 2-methoxy-6-vinylnaphthalene (final, 10 mM) as a sub-
42 strate. The reaction condition was optimized by detecting the
43 diol product with reverse-phase HPLC (Table S7). The dihy-
44 droxylation reaction proceeded very efficiently under an acid-
45 ic conditions (pH 2.0, at 70 °C for 5 h, Table S7) to give the
46 corresponding diol (LC yield, 92 %) together with a small
47 amount of over-oxidation product, aldehyde. By decreasing
48 the catalytic amount of Os-TM1459 to 0.01 mol % and in-
49 creasing the substrate concentration to 50 mM, a high TON of
50 9100 was obtained after 12 h (Table S8), indicating the ro-
51 bustness of the catalyst (LC yield, 91 %). The TON are compa-
52 rable or even higher than those of the *cis*-dihydroxylation
53 reaction catalyzed by the Os-complexes; the Os-TPA complex
54 system³⁰ and the Os-N4 complex system (N4 = *N,N'*-dimethyl-
55 2,11-diaza[3.3](2,6)pyridinophane)⁴² showed maximum TON
56 of 2500 and 5500 in cyclohexene dihydroxylation, respective-
57 ly. Thus, the results clearly illustrate that Os-TM1459 acts as a
58 peroxygenase with the high catalytic performance even under
59
60

such ill-suited conditions for “protein” (50 % organic solvent
and acidic pH, Figure S8B). Most of enzymes are hard to be
used in such a harsh conditions. Additionally, the enantiose-
lectivity is one of the most important issues of enzymatic
reactions. Unfortunately, however, enantioselectivity was
hardly observed in the present *cis*-dihydroxylation reaction. In
a docking simulation experiment using 2-methoxy-6-
vinylnaphthalene as a substrate, we found two low-energy
conformations with nearly the same energy (Figure S9AB).
This indicates that the wild type Os-TM1459 may not be able
to distinguish the *Si* and *Re* faces of the olefin substrates due
to the relatively large cavity size of this protein.

Taking the proposed reaction mechanism of Os-TPA for di-
hydroxylation of alkene into account,³⁰ a possible catalytic
mechanism by Os-TM1459 is shown in Scheme 2. First, **1** (Os-
TM1459) is oxidized with 1 equiv of H₂O₂ generating the ac-
tive species, oxo-hydroxo-Os(V) complex **2**, which reacts with
alkene via a concerted [3+2]-cycloaddition mechanism to
produce a five-membered glycolato-Os(III) intermediate **3**.
Finally, the hydrolyzation of **3** provides the starting complex **1**
as well as the corresponding diol product, completing the
catalytic cycle.

Catalytic *cis*-1,2-Dihydroxylation of Alkenes in a Preparative Scale. With intent to explore the catalytic performance of Os-TM1459 for organic synthesis, the reactions were examined in a preparative scale using various substrates (Table 1). Yields and stereochemistry of the diol products were determined by ¹H NMR by comparing that of authentic samples. Styrene and α -methylstyrene were efficiently converted to the corresponding diols in good yields (entries 1 and 2). The product yields somewhat decreased in the reaction of β -methylstyrene (*trans* and *cis*) and 2-methyl-1-phenylpropene (entries 3–5). It should be noted that only the *threo* and *erythro* products were obtained from the *trans*- and *cis*-styrene derivatives, respectively, suggesting that the reactions proceeded completely through *syn*-addition. When a styrene with even electron-withdrawing substituent (methyl cinnamate) was employed, the yield still retained a good level (entry 6).

Scheme 2. Proposed Reaction Mechanism for the Catalytic Dihydroxylation of Alkenes by Os-TM1459

**Table1. Catalytic *cis*-Dihydroxylation of Styrene Derivatives**

entry	substrate	product	¹ H NMR yield (%) ^a
1 ^b			78
2			90
3			59
4			68
5			53
6			55

^a ¹H NMR yield based on the substrate. ^b Reaction conditions: Os-TM1459 (2 mol%), substrate (25 mM), and H₂O₂ (25 mM) in 40 mM Britton-Robinson buffer / *t*-BuOH = 1/1 (v/v) at 70 °C for 5 h.

The yields of diol products were diminished by the substitution on β -position of styrene (Table 1). These results suggest that the steric effect induced by the protein matrix appears to govern the reaction efficiency rather than electronic effect. To confirm this, the reactions were conducted by using octene derivatives as substrate. In this case as well, only the *threo* and *erythro* products were obtained from the *trans*- and *cis*-octene derivatives, respectively (Table 2). It has been reported that simple OsO₄/H₂O₂ system exhibited the reaction yields that could be controlled via electronic effect (18 and 34 % for *trans*-2-octene and *trans*-4-octene, respectively, Table S9),⁴³ whereas Os-TPA showed the opposite tendency (83 and 55 % for *trans*-2-octene and *trans*-4-octene, respectively) due to the steric effects of the TPA ligand (Table S9).³⁰

However, much sharper substrate selectivity was observed in the case of Os-TM1459. Namely, the diol yield drastically decreased as the position of C=C double bond changed from 1-alkene to 4-alkene (75→24 %, Table 2, entries 1–4). Furthermore, such a simple tendency of substrate reactivity (1-octene > 2-octene > 3-octene > 4-octene) was not observed even in the case of Os-TPA system (1-octene \cong 2-octene > 3-octene \cong 4-octene, Table S9). Thus, Os-TM1459 system (75→24 % (3.1 fold) from 1- to 4-alkene) exhibited the sharper preference than Os-TPA system (90→55 %, 1.6 fold), suggesting that the steric effect is predominant in the case of Os-TM1459. In support of this notion, Os-TM1459 system preferred less sterically hindered *cis*-derivative to *trans*-derivative (58 vs 24 % (2.4 fold) for *cis* vs *trans*-4-octene) more prominently than Os-TPA system (74 vs 55 % (1.3 fold)). These results clearly demonstrated that the protein matrix magnifies the substrate selectivity in the Os-catalyzed *cis*-dihydroxylation reaction. This has been also confirmed by the docking simulation (Figure S9CD).

Table2. Catalytic *cis*-Dihydroxylation of *n*-Octene (n = 1, 2, 3, 4)

entry	substrate	product	¹ H NMR yield (%) ^a
1 ^b			75
2			52
3			33
4			24
5			79
6			58

^a ¹H NMR yield based on the substrate. ^b Reaction conditions: Os-TM1459 (2 mol%), substrate (25 mM) and H₂O₂ (25 mM) in 40 mM Britton-Robinson buffer / *t*-BuOH = 1/1 (v/v) at 70 °C for 5 h.

It has been reported that the diol yield decreased drastically, if H₂O₂ is added to the reaction solution at once in the case of Fe-complex⁴⁴ as well as Os-TPA.³⁰ Thus, to obtain higher product yields, H₂O₂ should be added slowly using a syringe pump or dropwise iteratively. This is presumably due to a catalase type disproportionation of H₂O₂ to O₂ and H₂O catalyzed by the metal center involved in the catalytic cycle. However, such a yield decrement was not observed in the Os-TM1459 system. Namely, the steric effect of protein scaffold and/or the interaction with the second coordination sphere of the protein matrix are probably responsible for the suppression of catalase-like activity by preventing the intermolecular decomposition of active species with H₂O₂ (Figure

S10). Such a hydrogen-bonding network in the second coordination sphere of protein matrix (Figure 4A), on the other hand, may prohibit substrate access to the Os-center, suppressing the intrinsic reactivity of the reactive oxidant. Therefore, the site-directed mutagenesis into the surrounding amino acid should lead to the improvement of catalytic activity.

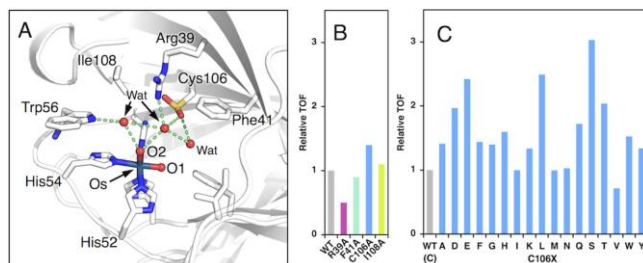


Figure 4. (A) Amino acid residues and hydrogen bonds around Os center in Os-TM1459. The protein main chain is displayed as white ribbon and key amino acid residues are highlighted as sticks. Hydrogen bonds are indicated in dotted green lines. (B) Relative catalytic activity (turnover frequencies (TOF)) of R39A, F41A, C106A, and I108A mutants. (C) Comparison of relative activity among C106X mutants.

Improvement of Peroxygenase Activity of Os-TM1459 by Site-targeted Mutagenesis. In order to examine the involvement of the neighboring amino acids in the catalysis, brief alanine-scanning mutagenesis was conducted toward the amino acids surrounding the Os center (Arg39, Phe41, Cys106, and Ile108, Figure 4AB, and Figure S11 and S12). The kinetic analysis on the dihydroxylation of 2-methoxy-6-vinylnaphthalene catalyzed by the wild type (WT) and these four mutants were performed by following the fluorescence of 2-methoxy-6-naphthalaldehyde derived by the post-treatment of the diol product with NaIO_4 . Such property will provide us the simple method in screening the catalytic activity of TM1459 variants.^{45,46} The amount of the product increased linearly during the initial several hours and then gradually slowed down to reach a plateau after 24 h (Figure S13). Then, the relative catalytic activity was evaluated using TOF determined from the initial straight line portion of the plot. As shown in Figure 4B, F41A and I108A mutants exhibited nearly the same reactivity, whereas R39A showed about 50 % activity when compared with WT. These results are indicative of the positive influence of the hydrogen bond network (Figure 4A). Concerning Cys106, C106A mutant showed 1.5-fold higher activity, probably because oxidized thiol group (sulfinate/sulfonate) cause a negative influence (see Figure S4 and S5). Thus, this position 106 was selected as a point for further site-directed mutagenesis investigation. The results are summarized in Figure 4C. Except the two mutants, C106R and C106P, which formed inclusion bodies, C106X mutants showed comparable to higher catalytic activity as compared to WT. Especially, the TOF values of C106E, C106L, and C106S were larger than that of WT by 2.5-, 2.5-, and 3-fold, respectively. Furthermore, C106S mutant showed similar substrate selectivity to that of WT in the preparative scale reaction (Table S9). This supports that enhancement of the intrinsic reactivity of the Os center could be possible without the influence on the interaction with olefin substrate by site-directed mutagenesis.

CONCLUSION

In this work, TM1459 cupin superfamily protein from *T. maritima* has been demonstrated to be a suitable scaffold for developing an artificial metalloenzyme. It should be noted that cupins belong to one of the most functionally diverse protein superfamily,⁴⁷ interestingly, in which many metalloproteins have occurred and the various sorts of first coordination spheres have been identified.⁴⁸ Therefore, many cupins will be highlighted as hopefully versatile ligands. In addition, TM1459 has no additional histidines except metal-coordinating four histidines. As a result, any non-specific binding of Os ion to this protein was not seen in ICP-AES and X-ray crystallographic analysis, and Os-TM1459 is able to catalyze *cis*-dihydroxylation of alkenes with the high TON. Constructing a well-defined complex of Os with protein led to the enhancement of thermal stability of protein folding and allowed us structure-based improvement of the catalytic activity retaining the substrate selectivity. Such enzyme repurposing strategy (metal substitution based on the metal binding promiscuity) can be confidently expanded as a promising means to explicit the power of platinum group elements as well as to acquire the robust enzyme scaffold. The compatibility with the improvement of catalytic activity based on the site-directed mutagenesis suggests that directed evolution strategies might be used to further optimize its performance.

ASSOCIATED CONTENT

Supporting Information

Experimental section; supporting figures and tables (PDF). The Supporting Information is available free of charge via the Internet at <http://pubs.acs.org>.

AUTHOR INFORMATION

Corresponding Author

fujieda@mls.eng.osaka-u.ac.jp (NF) and shinobu@mls.eng.osaka-u.ac.jp (SI)

Author Contributions

The manuscript was written through contributions of all authors. All authors have given approval to the final version of the manuscript.

Notes

The authors declare no competing financial interest.

ACKNOWLEDGMENT

N.F. thanks JSPS and MEXT, Japan (JSPS KAKENHI Grant Number JP15K13743 and MEXT KAKENHI Grant Number JP15H01066 in Hadean Bioscience, JP16H01025 in Precisely Designed Catalysts with Customized Scaffolding). S.I. thanks JST (the CREST program, 161052502). We thank Dr. K. Oohora and Dr. T. Hayashi for their kind assistance with ESI-MS, and Dr. E. Yamashita, Dr. A. Higashiura, and Dr. A. Nakagawa of SPring-8 BL-44XU for their support crystallographic data collection. This work was performed in part using a synchrotron beamline BL44XU at SPring-8 under the Cooperative Research Program of Institute for Protein Research, Osaka University. Diffraction data were collected at the Osaka University beamline BL44XU at SPring-8 (Harima, Japan) under proposal numbers 2014A6500, 2014B6500, 2015A6500, and 2015B6500.

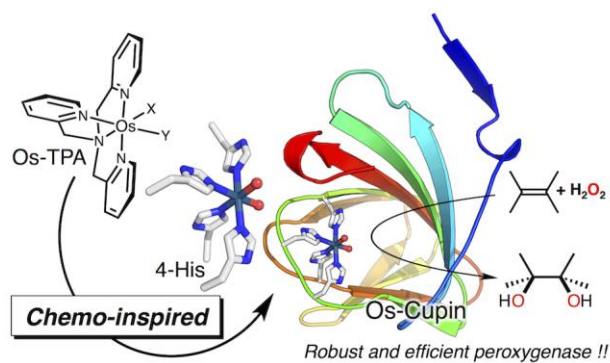
ABBREVIATIONS

T. maritima, *Thermotoga maritima*; *E. coli*, *Escherichia coli*; *t*-BuOH, tertiary-butylalcohol; TPA, tris(2-pyridylmethyl)amine; DSC, differential scanning calorimetry; CD, circular dichroism, HEPES, 4-(2-hydroxyethyl)-1-piperazineethanesulfonic acid; ICP-AES, Inductively Coupled Plasma-Atomic Emission Spectrometry; WT, wild type.

REFERENCES

- (1) Bornscheuer, U. T.; Huisman, G. W.; Kazlauskas, R. J.; Lutz, S.; Moore, J. C.; Robins, K. *Nature* **2012**, *485*, 185.
- (2) Ward, T. R. *Chem. Eur. J.* **2005**, *11*, 3798.
- (3) Boersma, A. J.; Megens, R. P.; Feringa, B. L.; Roelfes, G. *Chem. Soc. Rev.* **2010**, *39*, 2083.
- (4) Park, S.; Sugiyama, H. *Angew. Chemie Int. Ed.* **2010**, *49*, 3870.
- (5) Köhler, V.; Wilson, Y. M.; Lo, C.; Sardo, A.; Ward, T. R. *Curr. Opin. Biotechnol.* **2010**, *21*, 744.
- (6) Heinisch, T.; Ward, T. R. *Curr. Opin. Chem. Biol.* **2010**, *14*, 184.
- (7) Yu, F.; Cangelosi, V. M.; Zastrow, M. L.; Tegoni, M.; Plegaria, J. S.; Tebo, A. G.; Mocny, C. S.; Ruckthong, L.; Qayyum, H.; Pecoraro, V. L. *Chem. Rev.* **2014**, *114*, 3495.
- (8) Bos, J.; Roelfes, G. *Curr. Opin. Chem. Biol.* **2014**, *19*, 135.
- (9) Matsuo, T.; Hirota, S. *Bioorg. Med. Chem.* **2014**, *22*, 5638.
- (10) Hoarau, M.; Hureau, C.; Gras, E.; Faller, P. *Coord. Chem. Rev.* **2016**, *308*, 445.
- (11) Pàmies, O.; Diéguez, M.; Bäckvall, J.-E. *Adv. Synth. Catal.* **2015**, *357*, 1567.
- (12) Jeschek, M.; Reuter, R.; Heinisch, T.; Trindler, C.; Klehr, J.; Panke, S.; Ward, T. R. *Nature* **2016**, *537*, 661.
- (13) Key, H. M.; Dydio, P.; Clark, D. S.; Hartwig, J. F. *Nature* **2016**, *534*, 534.
- (14) Dydio, P.; Key, H. M.; Nazarenko, A.; Rha, J. Y.-E.; Seyedkazemi, V.; Clark, D. S.; Hartwig, J. F. *Science* **2016**, *354*, 102.
- (15) Ueno, T.; Tabe, H.; Tanaka, Y. *Chem. Asian J.* **2013**, *8*, 1646.
- (16) Lewis, J. C. *Curr. Opin. Chem. Biol.* **2015**, *25*, 27.
- (17) Song, W. J.; Tezcan, F. A. *Science* **2014**, *346*, 1525.
- (18) Fujieda, N.; Schätti, J.; Stutfeld, E.; Ohkubo, K.; Maier, T.; Fukuzumi, S.; Ward, T. R. *Chem. Sci.* **2015**, *6*, 4060.
- (19) Bornscheuer, U. T.; Kazlauskas, R. J. *Angew. Chemie Int. Ed.* **2004**, *43*, 6032.
- (20) Pordea, A. *Curr. Opin. Chem. Biol.* **2015**, *25*, 124.
- (21) Engeseth, H. R.; McMillin, D. R. *Biochemistry* **1986**, *25*, 2448.
- (22) Okrasa, K.; Kazlauskas, R. J. *Chemistry* **2006**, *12*, 1587.
- (23) Fernández-Gacio, A.; Codina, A.; Fastrez, J.; Riant, O.; Soumillion, P. *Chembiochem* **2006**, *7*, 1013.
- (24) Jing, Q.; Okrasa, K.; Kazlauskas, R. J. *Chem. Eur. J.* **2009**, *15*, 1370.
- (25) Jing, Q.; Kazlauskas, R. J. *ChemCatChem* **2010**, *2*, 953.
- (26) Key, H. M.; Clark, D. S.; Hartwig, J. F. *J. Am. Chem. Soc.* **2015**, *137*, 8261.
- (27) Jaroszewski, L.; Schwarzenbacher, R.; von Delft, F.; McMullan, D.; Brinen, L. S.; Canaves, J. M.; Dai, X.; Deacon, A. M.; DiDonato, M.; Elsliger, M.-A.; Eshagi, S.; Floyd, R.; Godzik, A.; Grittini, C.; Grzechnik, S. K.; Hampton, E.; Levin, I.; Karlak, C.; Klock, H. E.; Koesema, E.; Kovarik, J. S.; Kreuzsch, A.; Kuhn, P.; Lesley, S. A.; McPhillips, T. M.; Miller, M. D.; Morse, A.; Moy, K.; Ouyang, J.; Page, R.; Quijano, K.; Reyes, R.; Rezezadeh, F.; Robb, A.; Sims, E.; Spragggon, G.; Stevens, R. C.; van den Bedem, H.; Velasquez, J.; Vincent, J.; Wang, X.; West, B.; Wolf, G.; Xu, Q.; Hodgson, K. O.; Wooley, J.; Wilson, I. A. *Proteins Struct. Funct. Bioinforma.* **2004**, *56*, 611.
- (28) Hajnal, I.; Faber, K.; Schwab, H.; Hall, M.; Steiner, K. *Adv. Synth. Catal.* **2015**, *357*, 3309.
- (29) Que, L.; Tolman, W. B. *Nature* **2008**, *455*, 333.
- (30) Sugimoto, H.; Kitayama, K.; Mori, S.; Itoh, S. *J. Am. Chem. Soc.* **2012**, *134*, 19270.
- (31) Kokubo, T.; Sugimoto, T.; Uchida, T.; Tanimoto, S.; Okano, M. *J. Chem. Soc., Chem. Commun.* **1983**, 769.
- (32) Köhler, V.; Mao, J.; Heinisch, T.; Pordea, A.; Sardo, A.; Wilson, Y. M.; Knörr, L.; Creus, M.; Prost, J.; Schirmer, T.; Ward, T. R. *Angew. Chemie Int. Ed.* **2011**, *50*, 10863.
- (33) Konieczny, S.; Leurs, M.; Tiller, J. C. *ChemBioChem* **2015**, *16*, 83.
- (34) Meeuwissen, J.; Reek, J. N. H. *Nat. Chem.* **2010**, *2*, 615.
- (35) Prier, C. K.; Arnold, F. H. *J. Am. Chem. Soc.* **2015**, *137*, 13992.
- (36) Mayboroda, A.; Rheinwald, G.; Lang, H. *Inorganica Chim. Acta* **2003**, *355*, 69.
- (37) Dobson, J. C.; Takeuchi, K. J.; Pipes, D. W.; Geselowitz, D. A.; Meyer, T. J. *Inorg. Chem.* **1986**, *25*, 2357.
- (38) Mizutani, K.; Mikami, B.; Aibara, S.; Hirose, M. *Acta Crystallogr. Sect. D Biol. Crystallogr.* **2005**, *61*, 1636.
- (39) Lisi, G. P.; Hughes, R. P.; Wilcox, D. E. *J. Biol. Inorg. Chem.* **2016**, *21*, 659.
- (40) Ma, J. K.; Bishop, G. R.; Davidson, V. L. *Arch. Biochem. Biophys.* **2005**, *444*, 27.
- (41) Sugimoto, H.; Matsunami, C.; Koshi, C.; Yamasaki, M.; Umakoshi, K.; Sasaki, Y. *Bull. Chem. Soc. Jpn.* **2001**, *74*, 2091.
- (42) Sugimoto, H.; Ashikari, K.; Itoh, S. *Chem. Asian J.* **2013**, *8*, 2154.
- (43) Bergstad, K.; Jonsson, S. Y.; Bäckvall, J.-E. *J. Am. Chem. Soc.* **1999**, *121*, 10424.
- (44) Chen, M. S.; White, M. C. *Science* **2007**, *318*, 783.
- (45) List, B.; Barbas, C. F.; Lerner, R. a. *Proc. Natl. Acad. Sci.* **1998**, *95*, 15351.
- (46) Wahler, D.; Badalassi, F.; Crotti, P.; Reymond, J. *Chem. Eur. J.* **2002**, *8*, 3211.
- (47) Dunwell, J. M.; Purvis, A.; Khuri, S. *Phytochemistry* **2004**, *65*, 7.
- (48) Chavez, F.; Banerjee, A.; Slijivic, B. *Modeling the metal binding site in cupin proteins, On Biomimetics*; Pramatarova, L., Ed.; InTech: Rijeka, **2011**.

1
2 Authors are required to submit a graphic entry for the Table of Contents (TOC) that, in conjunction with the manuscript
3 title, should give the reader a representative idea of one of the following: A key structure, reaction, equation, concept, or
4 theorem, etc., that is discussed in the manuscript. Consult the journal's Instructions for Authors for TOC graphic specifica-
5
6



tions.

Insert Table of Contents artwork here